BJR

Received: 2 August 2013 | Revised: 9 September 2013 | Accepted: 3 October 2013

doi: 10.1259/bjr.20130481

Cite this article as:
Kim SM, Choi J-H, Chang S-A, Choe YH. Detection of ischaemic myocardial lesions with coronary CT angiography and adenosine-stress dynamic perfusion imaging using a 128-slice dual-source CT: diagnostic performance in comparison with cardiac MRI. Br J Radiol 2013;86: 20130481.

FULL PAPER

Detection of ischaemic myocardial lesions with coronary CT angiography and adenosine-stress dynamic perfusion imaging using a 128-slice dual-source CT: diagnostic performance in comparison with cardiac MRI

[1,2]S M KIM, MD, [2,3]J-H CHOI, MD, [2,3]S-A CHANG, MD and [1,2]Y H CHOE, MD

[1]Department of Radiology, Samsung Medical Center, Sungkyunkwan University School of Medicine, Seoul, Republic of Korea
[2]Cardiovascular Imaging Center, Samsung Medical Center, Sungkyunkwan University School of Medicine, Gangnam-gu, Seoul, Republic of Korea
[3]Division of Cardiology, Department of Medicine, Samsung Medical Center, Sungkyunkwan University School of Medicine, Seoul, Republic of Korea

Address correspondence to: Dr Yeon Hyeon Choe
E-mail: *yhchoe@skku.edu*

Objective: We assessed the diagnostic performance of adenosine-stress dynamic CT perfusion (ASDCTP) imaging and coronary CT angiography (CCTA) for the detection of ischaemic myocardial lesions using 128-slice dual-source CT compared with that of 1.5 T cardiac MRI.
Methods: This prospective study included 33 patients (61±8 years, 82% male) with suspected coronary artery diseases who underwent ASDCTP imaging and adenosine-stress cardiac MRI. Two investigators independently evaluated ASDCTP images in correlation with significant coronary stenosis on CCTA using two different thresholds of 50% and 70% diameter stenosis. Hypoattenuated myocardial lesions on ASDCTP associated with significant coronary stenoses on CCTA were regarded as true perfusion defects. All estimates of diagnostic performance were calculated and compared with those of cardiac MRI.
Results: With use of a threshold of 50% diameter stenosis on CCTA, the diagnostic estimates per-myocardial segment were as follows: sensitivity, 81% [95% confidence interval (CI): 70–92%]; specificity, 94% (95% CI: 92–96%); and accuracy 93% (95% CI: 91–95%). With use of a threshold of 70%, the diagnostic estimates were as follows: sensitivity, 48% (95% CI: 34–62%); specificity, 99% (95% CI: 98–100%); and accuracy, 94% (95% CI: 92–96%).
Conclusion: Dynamic CTP using 128-slice dual-source CT enables the assessment of the physiological significance of coronary artery lesions with high diagnostic accuracy in patients with clinically suspected coronary artery disease.
Advances in knowledge: Combined CCTA and ASDCTP yielded high accuracy in the detection of perfusion defects regardless of the threshold of significant coronary stenosis.

It is important to evaluate not only anatomical information about coronary arteries but also physiological information about myocardial perfusion for the precise assessment of coronary artery disease (CAD) [1]. Myocardial perfusion imaging (MPI) can provide haemodynamic information during exercise-induced or pharmacological stress. Single-photon emission tomography (SPECT), cardiac MRI or positron emission tomography (PET) has been extensively used for MPI [2,3]. Moreover, a normal MPI determined using these techniques carries an excellent prognosis with a low rate of cardiac events [4–6].

SPECT and PET are limited in their ability to evaluate coronary artery morphology and cardiac structures. By contrast, CT MPI with coronary CT angiography (CCTA) can evaluate not only anatomical structure, including coronary artery morphology, but also myocardial perfusion status. Although radiation dose associated with CT perfusion (CTP) is a concern, recent studies have shown that exposure to radiation can be reduced using different techniques, such as high-pitch helical scan of static CTP, half-scan duration of dynamic CTP and anatomical tube current modulation [7,8]. SPECT is more frequently used than MRI as a reference standard for evaluating the diagnostic accuracy of CTP. However, Jaarsma et al [9] reported that both cardiac MRI and PET showed a significantly higher diagnostic accuracy than SPECT for detection of obstructive CAD. Among several techniques of CTP, adenosine-stress dynamic CTP (ASDCTP) using 128-slice dual-source CT (DSCT) has the advantages of quantitative analysis of myocardial blood flow (MBF) and the use of

dynamic data sets [10–14]. There have been 2 previous studies of dynamic CTP using stress perfusion MRI as the reference standard [13,15], but these reports enrolled only 10 patients in the study arm evaluating dynamic CTP.

The purpose of this study was to evaluate the diagnostic performance of ASDCTP using a 128-slice DSCT for the detection of myocardial perfusion defects compared with adenosine-stress cardiac MRI.

METHODS AND MATERIALS

Patients

Our institutional review board approved this prospective study, and written informed consent was obtained from each patient. 33 patients with clinically suspected CAD were enrolled. They were referred to our unit for MPI using ASDCTP and cardiac MRI. The study included males and non-pregnant females who were older than 50 years and able to hold their breath during CT or MRI scan. The nature of the chest pain was evaluated with regard to three characteristics: (1) substernal pain, (2) whether the symptoms were precipitated by physical exertion or emotion and (3) whether prompt relief occurred within 10 min with rest or nitroglycerin. Typical angina was defined as presence of all of these characteristics. Atypical angina pectoris was defined as presence of two of the three characteristics. Non-anginal chest pain was characterised as presence of one or absence of the described features. The pre-test probability for obstructive CAD was estimated using the Duke Clinical Score, which included age, gender and character of chest discomfort [16,17]. Patients were categorised into low (1–30%), intermediate (31–70%) or high (71–99%) estimated pre-test probability. Exclusion criteria included poor renal function (serum creatinine >1.5 mg dl^{-1}), coronary artery bypass graft placement and haemodynamic and clinical instability (angina during rest, malignant arrhythmia). Patients were screened for contraindications to adenosine administration. Contraindications included second- or third-degree atrioventricular block without a functioning pacemaker, a history of asthma or severe obstructive lung disease, systolic blood pressure <90 mmHg, acute myocardial infarction or unstable coronary syndrome within 24 h after symptom onset, hypersensitivity to adenosine and intake of caffeine- or xanthine-containing compounds within the last 12 h. Metformin was discontinued at the time of CT imaging and was subsequently withheld for a minimum of 48 h in patients with an estimated glomerular filtration rate of <60 ml min^{-1} 1.73 m^{-2}. Beta-blockers and nitrates were discontinued prior to the CT examination.

CT protocol

All patients underwent cardiac CT using a DSCT system (SOMATOM Definition Flash; Siemens Medical Solutions, Forchheim, Germany) with $2\times64\times0.6$ mm detector collimation and the *z*-axis flying focal spot technique, resulting in 2×128 sections. Adenosine was infused in the left arm and contrast was injected in the right arm using bilateral antecubital intravenous catheters. Electrocardiography (ECG) leads were placed on the patient's chest, and a blood pressure cuff was placed on the patient's lower extremity. A detailed explanation of the CT examination with instructions for breath-holds was also included in patient preparation.

For calcium scoring, single-heartbeat CT scans were acquired with the following parameters: 280 ms gantry rotation time, 120 kV tube potential and 80 reference mAs per rotation tube current time product with the automatic tube current modulation technique (CARE Dose 4D; Siemens Medical Solutions).

Adenosine (0.14 mg kg^{-1} min^{-1}) infusion was then started for stress CTP, with monitoring of the patient's vital signs. Iodine contrast was also injected at 2 min and 54 s after the start of adenosine infusion with 40–50 ml of iomeprol 350 mg I ml^{-1}, followed by 40–50 ml of saline injected at 4–5 ml s^{-1}. The CTP scan was initiated at 3 min after the start of adenosine infusion and was performed in dynamic acquisition mode for 30 s, while maintaining adenosine infusion. Dynamic CTP was performed by shuttling the table between the two alternating table positions with ECG-triggered mode for every other R–R interval. The anatomical coverage of this imaging technique was 73 mm with a 10% overlap between both acquisition ranges for a given detector width of 38 mm. 100 kV tube voltage and automatic tube current modulation technique (CARE Dose 4D) with 350 reference mAs per rotation were used for dynamic stress scan.

After the ASDCTP scan, the adenosine infusion was discontinued immediately. This was followed by an interval of 5–10 min with monitoring of the patient's heart rate. When the patient's heart rate returned to baseline, CCTA was performed 1 min after sublingual administration of 0.4 mg of nitroglycerin. Beta-blockers were not administered before CCTA to reduce the time interval between stress CTP and rest CCTA. In our institute, oral beta-blockers are only available for use to patients undergoing CCTA. However, it takes at least 1 h to be effective. Retrospective ECG-gated helical mode scan was performed with the full radiation dose window set at 68–78% of the R–R interval in patients with heart rates ≤70 bpm or 200–400 ms after the R peak in patients with a heart rate of >70 bpm. The minimum tube current with 4% of the full radiation dose (MinDose®; Siemens Medical Solutions, Forchheim, Germany) was applied to the remainder of the R–R interval to minimise radiation dose. The typical contrast dose for CCTA was 70–80 ml of iomeprol 350 followed by 40 ml of saline at 4–5 ml s^{-1}. The CT scan was initiated 9 s after the bolus-tracking trigger was activated in the ascending aorta with a trigger threshold of 100 Hounsfield units. The acquisition parameters were $2\times64\times0.6$ mm detector collimation, resulting in $2\times128\times0.6$ mm sections, 280 ms gantry rotation time and 100 kV tube potential and 330 mAs per rotation tube current time product. The scan range was from above the origin of the coronary arteries to below the dome of the diaphragm in the craniocaudal direction.

Cardiac MRI

Cardiac MRI was performed using a 1.5 T unit (MAGNETOM Avanto; Siemens Medical Solutions, Erlangen, Germany). For stress MR perfusion imaging, adenosine was injected intravenously at 0.14 mg kg^{-1} min^{-1}) for 3 min before perfusion MRI and continued during perfusion MRI. Four short-axis slices (one each in the basal and apical levels, two in mid-ventricular levels) were obtained. Sequences were acquired immediately after the injection of gadobutrol (Gadovist®; Bayer Healthcare, Berlin, Germany) at 0.1 mmol per kilogram of body weight at an

injection rate of 4 ml s^{-1}, followed by a 40 ml saline flush. 10 min after stress perfusion imaging, a second bolus of 0.1 mmol kg^{-1} gadobutrol was injected, and rest perfusion images were obtained. Spoiled gradient echo techniques (Turbo-FLASH pulse sequences) were used for stress and rest sequences (repetition time/echo time, 2.2/1.08 ms; flip angle, 12°; saturation pre-pulse delay, 110 ms; matrix, 104×160; field of view, 320×292 mm; acquisition window, 120 ms; slice thickness, 8 mm).

After rest perfusion scans, delayed enhancement imaging was performed using Turbo-FLASH sequences (field of view, 292×360 mm; repetition time/echo time, 8.2/3.17 ms; inversion time, 250–350 ms; flip angle, 25°; matrix, 125×256; slice thickness, 6 mm). The inversion time was selected for each series according to a Look–Locker sequence to optimise myocardial nulling. The images were acquired in a continuous short-axis view.

Image analysis

CTP images were evaluated by two experienced investigators (one with 3 years and one with 4 years of ASDCTP experience), both of whom were blinded to each subject's clinical data and identifiers. Readers independently analysed the images. Discordant findings were reconciled during consensus reading. MR perfusion imaging was considered the reference standard for the detection of CTP defects. Two investigators, one with 3 years and one with 12 years of stress perfusion cardiac MRI experience, analysed the images for the presence of perfusion defects for consensus reading.

Diagnostic performance for the detection of myocardial perfusion defects

Dynamic stress CTP images were reconstructed at 280 ms of the R–R interval using a standard kernel (B23f). The stress images were read in the cardiac short-axis view at a 4-mm slice thickness with averaged reconstruction. The image quality of CTP images was visually assessed using a four-point scale (1 = poor, non-diagnostic image; 2 = fair, the presence of moderate artefacts which allow diagnosis; 3 = good, the presence of any artefacts which do not interfere with image interpretation; 4 = excellent, the absence of any artefacts). Grade 2–4 qualities were regarded as diagnostic. Artefacts included motion, beam-hardening, image reconstruction and misalignment artefacts. To detect subtle perfusion defects, observers used a user-defined narrow window width and window level setting as described previously [18]. Dynamic stress CT images were evaluated visually according to the 16 myocardial segments excluding the apical segment [19]. Myocardial segments were considered to show perfusion defects when hypoperfusion lasted for more than six heartbeats on dynamic data sets [13]. We excluded myocardial segments which covered ≤50% of the thickness of the myocardium because of limited scan coverage (73 mm).

We also evaluated the CCTA images simultaneously to differentiate true perfusion defects from artefacts. First, coronary artery stenosis was evaluated visually. Then, observers calculated the percentage of diameter stenosis on vessel cross-section images using commercial software (iNtuition™ v. 4.4.7; TeraRecon, Inc., Foster City, CA). Significant coronary artery stenosis was classified by two different thresholds (≥50% and ≥70% diameter stenosis) by using a modified 17-segment model of the coronary artery tree [13]. Among the vessel segments with degree of stenosis near the threshold, the stenotic lesions with blooming or motion artefacts were also considered as significant stenosis. Among myocardial segments with hypoattenuated lesions, only the segments associated with significant coronary stenoses were regarded as perfusion defects. The hypoattenuated segments without associated significant coronary stenoses were considered as artefacts. The results of the CTP images were compared with those of cardiac MRI. Myocardial segments were considered as showing perfusion defect when hypoperfusion lasted for more than 2 s compared with remote healthy myocardium and persisted for at least 10 frames on perfusion MRI [20].

Quantitative analysis of CT perfusion

A colour-coded map of CTP was generated using Volume Perfusion software (Leonardo™; Siemens Medical Solutions, Erlangen, Germany). The MBF and myocardial blood volume (MBV) were also calculated. A dedicated parametric deconvolution technique was used to fit the time-attenuation curves for quantitative analysis. A two-compartment model of intravascular and extravascular space was used for deconvolution [21]. To increase the precision of the fit, double sampling of the arterial input function (AIF) was conducted. The input function was sampled at every table position in the descending thoracic aorta and was integrated into one AIF. Therefore, AIF had double the sampling rate than the tissue time-attenuation curve. An algorithm was used to establish the maximum slope using the fit model curve for every voxel and measured MBF from the following relationship: MBF=maximum slope/maximum AIF, where the maximum slope indicates the tissue time-attenuation curve, and the maximum AIF indicates the maximum AIF value [13,18]. MBF and MBV were determined in each of the 16 myocardial segments, excluding the apical segment [19].

Radiation dose

The effective radiation dose was derived by multiplying the dose-length product (DLP) by the conservative constant k (k=0.014 mSv mGy^{-1} cm^{-1}) according to the standard methodology outlined in the European Guidelines on Quality Criteria for Computed Tomography [22].

Statistical analysis

All continuous data were expressed as mean ± standard deviation, whereas categorical variables were expressed as percentages. The diagnostic estimates of ASDCTP for the detection of perfusion defects, with cardiac MRI as the reference standard, were defined by sensitivity, specificity, positive predictive value, negative predictive value and accuracy; 95% confidence intervals (CIs) were provided for each estimate. Calculations were performed on a per-myocardial segment, a per-territory and a per-patient basis. For interobserver agreements, the Cohen's kappa value was used. All reported diagnostic values are based on consensus between the two observers. $p<0.05$ was considered to indicate statistical significance. Statistical analysis was performed using MedCalc® software (MedCalc, Mariakerke, Belgium).

RESULTS

Study population

All patients were examined using cardiac MRI within 1 month of ASDCTP (15±9 days; range, 0–30 days). Of the 33 patients

(mean age, 61±8 years), 27 (82%) patients were males, 23 (70%) patients had intermediate or high pre-test probability of CAD and 18 (55%) patients were former or current smokers. Patient characteristics are listed in Table 1.

CT scanning parameters

The CT scanning parameters are summarised in Table 2. The mean heart rate was 76±13 bmp at stress and 69±10 bmp at rest (p=0.01). Mean effective radiation dose for the stress acquisitions was 5.3±1.0 mSv and 376.4±71.2 DLP. The radiation dose of rest acquisitions was 4.0±0.7 mSv and 286.3±48.3 DLP. The mean total effective radiation exposure was 10.3±1.1 mSv and 735.8±78.7 DLP.

Diagnostic accuracy of combined CCTA and ASDCTP for the detection of perfusion defects

In the assessment of coronary artery stenosis on CCTA, the number of vessels with significant stenoses that were correlated with myocardial segments with hypoattenuation was as follows: 27 vessels (14 vessels with blooming artefacts), with the threshold of >50% diameter stenosis, and 10 vessels (2 vessels with blooming artefacts), with the threshold of >70% diameter stenosis. In the evaluation of ASDCTP, 6 (1%) basal anterior segments of 528 segments were excluded from the analysis because of the limited anatomical coverage of the axial shuttle scan mode. Therefore, a total of 522 (99%) segments were included in the analysis. In the evaluation of MRI, 13 (39%) of the 33 patients and 52 (10%) of the 522 segments had perfusion abnormalities. Among them, 10 (30%) patients and 45 (9%) segments had myocardial infarction on late gadolinium enhancement images. The diagnostic estimates of combined CCTA and ASDCTP in the detection of perfusion defects were calculated based on myocardial segments, territories and patients (Table 3).

Table 1. Baseline characteristics of 33 patients

Age (years)[a]	61±8
Male	27 (82%)
Body mass index (kg m^{-2})[a]	24.4±2.9
Body weight (kg)[a]	66.6±10.0
Pre-test probability of coronary artery disease	
Low probability	10 (30%)
Intermediate probability	18 (55%)
High probability	5 (15%)
Coronary risk profile	
Arterial HTN[b]	19 (58%)
Cigarette smoking	18 (55%)
Positive family history	7 (21%)
Dyslipidemia[c]	21 (64%)
Diabetes[d]	21 (64%)
Lipid level (mg dl^{-1})[a]	
Total cholesterol	161.5±30.8
High-density lipoprotein cholesterol	47.6±8.4
Low-density lipoprotein cholesterol	90.4±24.5
Serum triglyceride	132.5±59.4

HTN, hypertension.
Unless otherwise noted, data are numbers of patients. Coronary risk profile, diabetes and medical history were classified according to documentation in the cardiologist's notes.
[a]Mean value ± standard deviation.
[b]Diagnosis of HTN or blood pressure >140/90 or on medication for HTN.
[c]Diagnosis of dyslipidemia or medication for dyslipidemia, total cholesterol >200 mg dl^{-1} or low-density lipoprotein cholesterol >130 mg dl^{-1}.
[d]Diagnosis of diabetes mellitus or fasting blood sugar ≥126 mg dl^{-1} at least once or on medication for diabetes mellitus.

With a cut-off value of >50% diameter stenosis (Figure 1), 18 (55%) of the 33 patients and 71 (14%) of the 522 segments had perfusion abnormalities on ASDCTP images and concordant coronary stenoses on CCTA images. On segment-based analysis of ASDCTP images, 441 (84%) segments were true negative, 42 (8%) segments true positive (Figure 2), 10 (2%) segments false negative (Figure 3) and 29 (6%) segments false positive. False-positive segments were correlated with 13 significant coronary artery stenoses at CCTA: right coronary artery, n=3; left anterior descending (LAD), n=9; left circumflex, n=1. On patient-based analysis, 12 (36%) patients were true negative, 10 (30%) patients true positive, 3 (10%) patients false negative and 8 (24%) patients false positive. The three patients with false-negative results had two or three myocardial segments with perfusion defects, and two of the three patients had reversible myocardial ischaemia on cardiac MRI. By contrast, the 10 patients with true-positive results had 4±3 myocardial segments (range, 2–13 segments) with perfusion defects, and 9 of 10 patients had myocardial infarction on cardiac MRI.

With a cut-off value >70% diameter stenosis (Figure 1), 7 (21%) of the 33 patients and 30 (6%) of the 522 segments had perfusion abnormalities on ASDCTP images and concordant coronary stenoses on CCTA images. On segment-based analysis of ASDCTP images, 465 (89%) segments were true negative, 25 (5%) segments true positive, 27 (5%) segments false negative and 5 (1%) segments false positive. False-positive segments were correlated with 2 LAD stenoses at CCTA. On the patient-based analysis, 19 (58%) patients were true negative, 6 (18%) patients true positive, 7 (21%) patients false negative and 1 (3%) patient false positive. The 7 patients with false-negative results had 3±2 myocardial segments (range, 2–6 segments) with perfusion defects, and 5 of the 7 patients had myocardial infarction on cardiac MRI. By contrast, the 6 patients with true-positive results had 3±4 myocardial segments (range, 2–13 segments) with perfusion defects and 5 of the 6 patients had myocardial infarction on cardiac MRI.

In all the analyses with per-myocardial segment, per-territory and per-patient, sensitivities of threshold of 50% significant stenosis were higher than those of threshold of 70%. The specificities and overall diagnostic accuracies of threshold of 70% significant stenosis were higher than the threshold of 50% (Table 3).

Table 2. CT parameters

Parameter	Stress CT perfusion	Rest CTA
Heart rate (bmp)		
Minimum	58±15	67±11
Maximum	92±16	74±12
Mean	76±13	69±10
Scan mode	Axial shuttle	Helical
Tube voltage (kV)	100	100
Tube current (mAs)	350[a]	330
Effective radiation exposure (mSv)	5.3±1.0	4.0±0.7
Contrast		
Volume (ml)	48.3±3.5	76.4±6.0
Flow rate (ml s^{-1})	4.8±0.3	4.4±0.5

CTA, CT angiography.
Unless otherwise noted, data are mean values±standard deviation.
[a]350 reference mAs per rotation with tube current modulation (CARE Dose 4D; Siemens Medical Solutions, Forchheim, Germany).

Quantitative analysis of CT perfusion

Measurements of MBF and MBV are given in Table 4. 52 (10%) of the 522 segments included had perfusion abnormalities on cardiac MRI. Those segments were considered as true perfusion defects by quantitative analysis. The mean MBF of all myocardial segments during ASDCTP was 113.5±28.2 ml 100 ml^{-1} min^{-1}. There was a significant difference in the MBF values between normal (113.2±26.0 ml 100 ml^{-1} min^{-1}) and hypoperfused (62.4±21.8 ml 100 ml^{-1} min^{-1}) myocardial segments ($p<0.01$). The mean myocardial blood volume of all myocardial segments during ASDCTP was 19.8±3.3 ml 100 ml^{-1}. There was a significant difference in the myocardial blood volume values between normal (21.1±3.4 ml 100 ml^{-1}) and hypoperfused (13.2±5.5 ml 100 ml^{-1}) myocardial segments ($p<0.01$). Of the 52 segments with abnormal perfusion, 7 (15%) segments showed myocardial ischaemia and 45 (85%) segments showed myocardial infarction on cardiac MRI. There was a significant difference in the MBF values between ischaemic (78.2±7.6 ml 100 ml^{-1} min^{-1}) and infarcted (59.6±14.5 ml 100 ml^{-1} min^{-1}) myocardial segments ($p<0.01$).

Table 3. Diagnostic accuracy of combined coronary CT angiography and adenosine-stress dynamic CT perfusion for detection of ischaemic myocardial lesions with use of cardiac MRI as the reference standard

Estimates	Per-myocardial segment	Per-territory	Per-patient
Stenosis >50%			
Sensitivity	81 (42/52) [70–92]	82 (14/17) [64–100]	77 (10/13) [54–100]
Specificity	94 (441/470) [92–96]	84 (69/82) [76–92]	60 (12/20) [39–82]
PPV	59 (42/71) [48–70]	52 (14/27) [33–71]	56 (10/18) [33–79]
NPV	98 (441/451) [97–99]	96 (69/72) [92–100]	80 (12/15) [60–100]
Accuracy	93 (483/522) [91–95]	84 (83/99) [77–91]	67 (22/33) [51–83]
Stenosis >70%			
Sensitivity	48 (25/52) [34–62]	47 (8/17) [23–71]	46 (6/13) [19–73]
Specificity	99 (465/470) [98–100]	98 (80/82) [95–100]	95 (19/20) [85–100]
PPV	83 (25/30) [70–96]	80 (8/10) [55–100]	86 (6/7) [60–100]
NPV	95 (465/492) [93–97]	90 (80/89) [84–96]	73 (19/26) [56–90]
Accuracy	94(490/522) [92–96]	89 (88/99) [83–95]	76 (25/33) [61–91]

NPV, negative predictive value; PPV, positive predictive value.
All data are percentages. The absolute numbers used to calculate the percentages are in parentheses. Numbers in square brackets are 95% confidence intervals as percentages. Per-myocardial segment analysis was based on data from a total of 522 myocardial segments. Six segments were excluded from analysis because they were not covered by limited scan coverage. Per-territory analysis was based on data from a total of 99 territories. Per-patient analysis was based on data from a total of 33 patients.

Figure 1. Flow chart of analysis of adenosine-stress dynamic CT perfusion (ASDCTP) images. The results of ASDCTP were compared with those of MR perfusion. C, concordant; CAS, coronary artery stenosis; CCTA, coronary CT angiography; D, discordant; FN, false negative; FP, false positive; TN, true negative; TP, true positive.

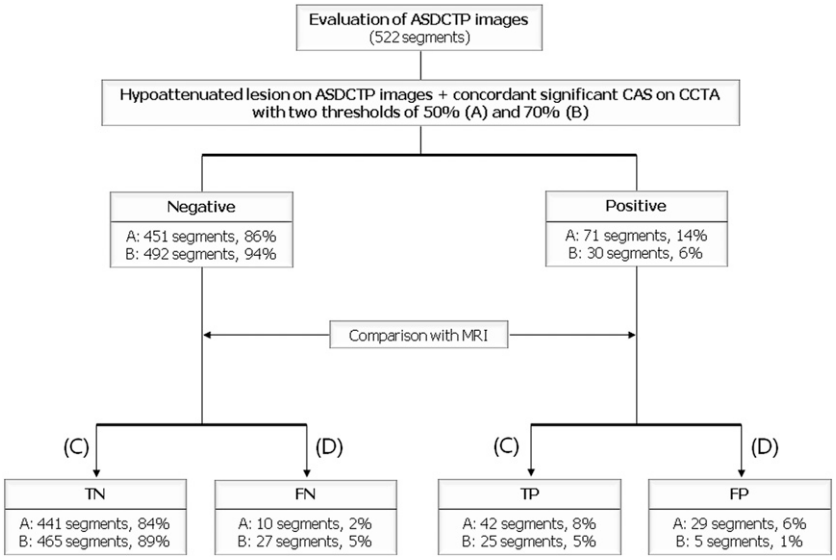

Image quality assessment and interobserver variability

On a patient-based image quality analysis of CTP images using a four-point scale, the median score was 3 (range, 2–4). All CTP images were defined as diagnostic. In the detection of perfusion defects, the agreement between the blinded independent readers regarding ASDCTP findings was 94% and the κ-value was 0.70.

DISCUSSION

We evaluated the diagnostic performances of ASDCTP using 128-slice DSCT for the detection of perfusion defects in comparison with cardiac MRI as the gold standard in 33 patients with clinically suspected CAD. Our data showed that sensitivity (81%) of combined CCTA and ASDCTP was higher than the threshold of ≥50% diameter stenosis on CCTA and their

Figure 2. Images of a 70-year-old male with unstable angina: (a) coronary CT angiography shows a significant stenosis in the proximal RCA (white arrow); (b) dynamic CT perfusion shows a hypoattenuated lesion (black arrow) in the inferior wall at the mid-ventricular level; (c) colour-coded map shows a perfusion defect in the right coronary artery territory (black arrows; colour visible in online version only); (d) on cardiac MRI, adenosine-stress perfusion shows low signal intensity (black arrows), indicating a subendocardial perfusion defect in the same myocardial segment; (e) there is no low-signal-intensity lesion on rest perfusion imaging; and (f) there is no myocardial infarction on delayed enhancement imaging.

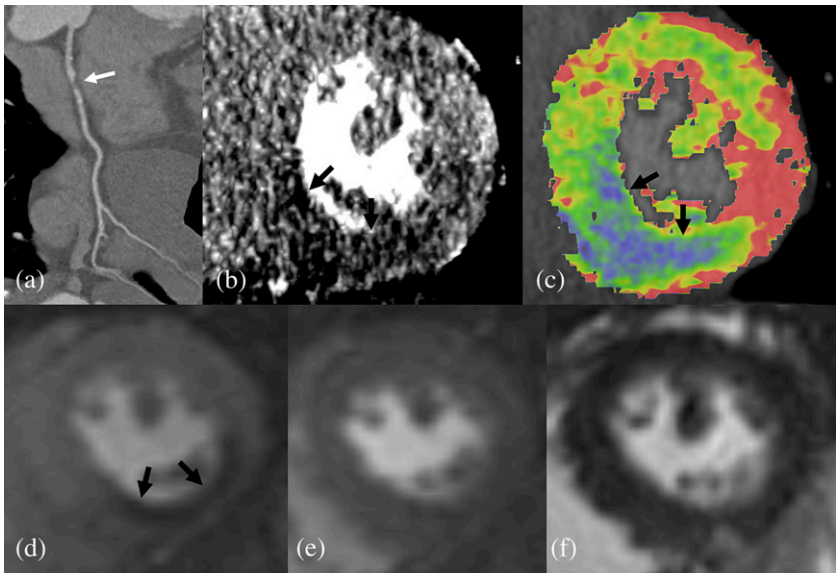

Figure 3. Images of a 53-year-old male with unstable angina: (a) coronary CT angiography shows a significant stenosis in the proximal left anterior descending (LAD) artery (white arrow); (b) dynamic CT perfusion shows no discrete hypo-attenuated lesion in the LAD territory; (c) there is no territorial perfusion defect on colour-coded map (colour visible in online version only); (d) on cardiac MRI, adenosine-stress perfusion shows an area of low signal intensity (black arrows), indicating a subendocardial perfusion defect in the LAD territory of mid-ventricular level; (e) there is no low-signal-intensity lesion on rest perfusion imaging; and (f) there is no myocardial infarction on delayed enhancement imaging.

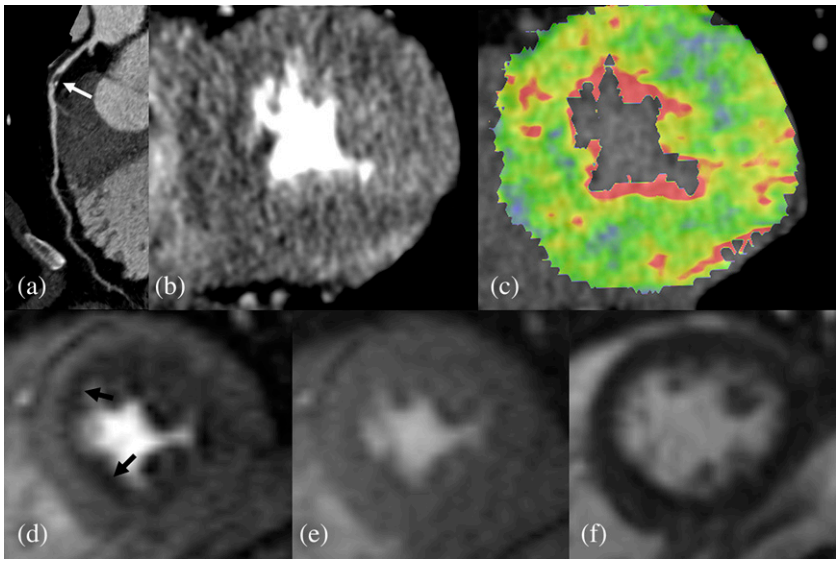

specificity (99%) was higher than the threshold of ≥70% diameter stenosis and the accuracies (≥93%) were higher than both thresholds. Recent studies have demonstrated the feasibility of adenosine-induced CTP using static or dynamic scanning for detecting perfusion defects compared with SPECT or cardiac MRI [7,13–15,23–28]. Among them, two studies of dynamic CTP using 128-slice DSCT reported high sensitivity (86.1%) and specificity (98.2%) compared with cardiac MRI as the reference standard [13,15]. However, only 10 patients were enrolled in each study.

Our results showed that sensitivity (81%) was relatively lower than 86.1% of previous studies [13,15]. It might be caused by inclusion of lesions with intermediate stenosis with artefacts. These lesions were classified as significant stenosis on CCTA. On the territory-based analysis, false-positive cases were frequently associated with LAD territories; 64% (9/13) with threshold of ≥50% diameter stenosis and 100% (2/2) with threshold of ≥70% diameter stenosis. This might be caused by scatter artefacts [29]. This artefact was noted in the septum, especially the basal anteroseptal wall between the left-ventricle and right-ventricle outflow tract. Application of scatter-correction algorithm to dynamic CTP may help interpret myocardial CTP images using current DSCT techniques [30].

The radiation dose is a major issue for clinical application of CTP. In dynamic CTP studies using 128-slice DSCT, effective radiation doses of stress scans ranged from 7.1 to 10.3 mSv and those of total CT scans (including CCTA or rest CTP) ranged from 12.8 to 18.1 mSv [13,14]. These radiation doses were calculated using a conversion factor of 0.014. This conversion factor was derived for general chest CT and may underestimate the radiation dose of cardiac imaging. Actually, Geleijns et al [31] proposed a conversion factor of 0.030 for cardiac imaging. Therefore, the reduction of radiation dose is more important for dynamic CTP. The radiation dose of our protocol was relatively lower than those of previous studies using dynamic CTP [13,14,26], because the automatic anatomical tube current modulation technique (CARE Dose 4D) was applied to stress CTP in our study. A recent study reported that dynamic CTP with this technique reduced the radiation dose by up to 36% compared with radiation exposure of fixed tube current [8]. Radiation dose may be decreased with static CTP, especially with ECG-pulsing tube current modulation or high-pitch technique. Feuchtner et al [7] demonstrated the feasibility of low-dose static CTP with a high-pitch helical mode. They reported that the mean effective radiation doses for the stress and rest acquisitions were 0.93 mSv and 1.59 mSv, respectively. The mean total effective radiation exposure was

Table 4. Quantitative analysis of CT perfusion

Parameter	Normal myocardium	Abnormal myocardium	Whole myocardium
MBF (ml 100 ml^{-1} min^{-1})	113.2±26.0	62.4±21.8	113.5±28.2
MBV (ml 100 ml^{-1})	21.1±3.4	13.2±5.5	19.8±3.3

MBF, myocardial blood flow for 100 ml of myocardium per minute; MBV, myocardial blood volume for 100 ml of myocardium.
Unless otherwise noted, data are mean values ± standard deviation.

2.50 mSv. Using single static CTP techniques, cardiac motion artefacts associated with high heart rates during adenosine stress may not be easily discriminated from true perfusion defects. Although dynamic CTP yields a higher radiation dose than static CTP, its advantages include the ability to generate dynamic data sets for visual analysis of serial dynamic images and quantitative analysis of MBF. For its widespread use, further studies are needed to reduce the radiation dose of dynamic CTP.

Previous studies [12–14,32] reported that the MBFs of normal myocardium ranged from 104.8 to 142.9 ml 100 ml^{-1} min^{-1} and the MBFs of hypoperfused myocardium ranged from 52.0 to 96.0 ml 100 ml^{-1} min^{-1}. Bamberg et al [12] also reported that the presence of coronary stenosis with a corresponding MBF $<$75 ml 100 ml^{-1} min^{-1} indicated a high risk of haemodynamic significance. Further studies are needed to determine the threshold MBF values for myocardial ischaemia for quantitative analysis of CTP.

Our study had some limitations. First, because only four slices of perfusion MRI were available for analysis using current technology, we could not compare the whole myocardium between CTP and perfusion MRI. Second, we started CT or MRI scanning just after adenosine infusion for around 3 min and could not record the objective evidences of stress expressed by the patients' reactions to the adenosine infusion in the remaining part of adenosine infusion during the examinations. We only monitored the patients' conditions during adenosine infusion. The third limitation is that we could not compare absolute quantification of MBF between CTP and perfusion MRI. Fourth, the scan duration of dynamic CTP was 30 s. This might be too long for some symptomatic patients to hold their breath completely. Therefore, a shorter scan duration of dynamic CTP should be adopted or motion correction algorithm of dynamically acquired images should be developed to reduce respiratory motion artefact. Fifth, only low-attenuated lesions associated with significant epicardial coronary artery stenoses were considered as true perfusion defects in this study. The use of this definition might miss perfusion defects caused by microvascular disease. Sixth, selection bias in patient recruitment might be present in our study. We did not include the patients on the grounds of their pre-test probability of CAD. A large proportion of myocardial segments had no perfusion defects on ASDCTP. Thus, the results are only comparable to a population with a similar prevalence of CAD as in our result. Also, we did not separate and compare the estimates of diagnostic accuracy for the detection of reversible and fixed perfusion defects. Our CT protocol did not include delayed enhancement scan, which might be useful to differentiate myocardial infarction from myocardial ischaemia. Rest CCTA provided the information such as myocardial thinning or subendocardial fat infiltration, and it might be helpful in discriminating myocardial infarction. However, in our data, there were only several myocardial segments (1%, 7/522) with reversible myocardial ischaemia. The last limitation of this study is that this study was a single-institution study and the number of patients was relatively small.

CONCLUSIONS

Our results show that the overall diagnostic accuracies of the combined CCTA and ASDCTP imaging are 93% and 94% in comparison with adenosine-stress cardiac MRI with thresholds of 50% and 70% diameter stenosis on CCTA, respectively. Our findings support that dynamic CTP using 128-slice DSCT may enable the functional testing of stenotic coronary vessels in patients with clinically manifested CAD. Further technical improvements for dynamic CTP using DSCT are required to reduce artefacts and radiation dose for widespread clinical use of this technique.

FUNDING

This study was supported by a grant from Korea Health Technology R&D Project, Ministry for Health, Welfare & Family Affairs, Republic of Korea (A102065-26).

REFERENCES

1. Smith SC Jr, Feldman TE, Hirshfeld JW Jr, Jacobs AK, Kern MJ, King SB 3rd, et al. ACC/AHA/SCAI 2005 guideline update for percutaneous coronary intervention: a report of the American College of Cardiology/American Heart Association Task Force on Practice Guidelines (ACC/AHA/SCAI Writing Committee to Update 2001 Guidelines for Percutaneous Coronary Intervention). Circulation 2006;113:e166–286.
2. Hachamovitch R, Berman DS, Kiat H, Cohen I, Cabico JA, Friedman J, et al. Exercise myocardial perfusion SPECT in patients without known coronary artery disease: incremental prognostic value and use in risk stratification. Circulation 1996;93:905–14.
3. Schwitter J, Nanz D, Kneifel S, Bertschinger K, Buchi M, Knusel PR, et al. Assessment of myocardial perfusion in coronary artery disease by magnetic resonance: a comparison with positron emission tomography and coronary angiography. Circulation 2001;103:2230–5.
4. Lerakis S, McLean DS, Anadiotis AV, Janik M, Oshinski JN, Alexopoulos N, et al. Prognostic value of adenosine stress cardiovascular magnetic resonance in patients with low-risk chest pain. J Cardiovasc Magn Reson 2009;11:37. doi: 10.1186/1532-429X-11-37
5. Metz LD, Beattie M, Hom R, Redberg RF, Grady D, Fleischmann KE. The prognostic value of normal exercise myocardial perfusion imaging and exercise echocardiography: a meta-analysis. J Am Coll Cardiol 2007;49:227–37. doi: 10.1016/j.jacc.2006.08.048
6. Yoshinaga K, Chow BJ, Williams K, Chen L, deKemp RA, Garrard L, et al. What is the prognostic value of myocardial perfusion imaging using rubidium-82 positron emission tomography? J Am Coll Cardiol 2006;48:1029–39. doi: 10.1016/j.jacc.2006.06.025
7. Feuchtner G, Goetti R, Plass A, Wieser M, Scheffel H, Wyss C, et al. Adenosine stress high-pitch 128-slice dual-source myocardial computed tomography perfusion for imaging of reversible myocardial ischemia: comparison with magnetic resonance imaging. Circ Cardiovasc Imaging 2011;4:540–9.
8. Kim SM, Kim YN, Choe YH. Adenosine-stress dynamic myocardial perfusion imaging using 128-slice dual-source CT: optimization of the CT protocol to reduce the radiation dose. Int J Cardiovasc Imaging 2013;29:875–84. doi: 10.1007/s10554-012-0138-x

9. Jaarsma C, Leiner T, Bekkers SC, Crijns HJ, Wildberger JE, Nagel E, et al. Diagnostic performance of noninvasive myocardial perfusion imaging using single-photon emission computed tomography, cardiac magnetic resonance, and positron emission tomography imaging for the detection of obstructive coronary artery disease: a meta-analysis. J Am Coll Cardiol 2012;59: 1719–28.
10. Bamberg F, Hinkel R, Schwarz F, Sandner TA, Baloch E, Marcus R, et al. Accuracy of dynamic computed tomography adenosine stress myocardial perfusion imaging in estimating myocardial blood flow at various degrees of coronary artery stenosis using a porcine animal model. Invest Radiol 2012; 47:71–7.
11. Ho KT, Chua KC, Klotz E, Panknin C. Stress and rest dynamic myocardial perfusion imaging by evaluation of complete time-attenuation curves with dual-source CT. JACC Cardiovasc Imaging 2010;3:811–20. doi: 10.1016/j.jcmg.2010.05.009
12. Bamberg F, Becker A, Schwarz F, Marcus RP, Greif M, von Ziegler F, et al. Detection of hemodynamically significant coronary artery stenosis: incremental diagnostic value of dynamic CT-based myocardial perfusion imaging. Radiology 2011;260: 689–98.
13. Bastarrika G, Ramos-Duran L, Rosenblum MA, Kang DK, Rowe GW, Schoepf UJ. Adenosine-stress dynamic myocardial CT perfusion imaging: initial clinical experience. Invest Radiol 2010;45:306–13. doi: 10.1097/RLI.0b013e3181dfa2f2
14. Wang Y, Qin L, Shi X, Zeng Y, Jing H, Schoepf UJ, et al. Adenosine-stress dynamic myocardial perfusion imaging with second-generation dual-source CT: comparison with conventional catheter coronary angiography and SPECT nuclear myocardial perfusion imaging. AJR Am J Roentgenol 2012;198: 521–9. doi: 10.2214/AJR.11.7830
15. Weininger M, Schoepf UJ, Ramachandra A, Fink C, Rowe GW, Costello P, et al. Adenosine-stress dynamic real-time myocardial perfusion CT and adenosine-stress first-pass dual-energy myocardial perfusion CT for the assessment of acute chest pain: initial results. Eur J Radiol 2012;81:3703–10. doi: 10.1016/j.ejrad.2010.11.022
16. Gibbons RJ, Balady GJ, Bricker JT, Chaitman BR, Fletcher GF, Froelicher VF, et al. ACC/AHA 2002 guideline update for exercise testing: summary article: a report of the American College of Cardiology/American Heart Association Task Force on Practice Guidelines (Committee to Update the 1997 Exercise Testing Guidelines). Circulation 2002;106:1883–92.
17. Pryor DB, Shaw L, McCants CB, Lee KL, Mark DB, Harrell FE Jr, et al. Value of the history and physical in identifying patients at increased risk for coronary artery disease. Ann Intern Med 1993;118:81–90.
18. Mahnken AH, Klotz E, Pietsch H, Schmidt B, Allmendinger T, Haberland U, et al. Quantitative whole heart stress perfusion CT imaging as noninvasive assessment of hemodynamics in coronary artery stenosis: preliminary animal experience. Invest Radiol 2010;45:298–305. doi: 10.1097/RLI.0b013e3181dfa3cf
19. Cerqueira MD, Weissman NJ, Dilsizian V, Jacobs AK, Kaul S, Laskey WK, et al. Standardized myocardial segmentation and nomenclature for tomographic imaging of the heart: a statement for healthcare professionals from the Cardiac Imaging Committee of the Council on Clinical Cardiology of the American Heart Association. Circulation 2002;105:539–42.
20. Taylor AJ, Al-Saadi N, Abdel-Aty H, Schulz-Menger J, Messroghli DR, Friedrich MG. Detection of acutely impaired microvascular reperfusion after infarct angioplasty with magnetic resonance imaging. Circulation 2004;109:2080–5. doi: 10.1161/01.CIR.0000127812.62277.50
21. Bruder H, Raupach R, Klotz E, Stierstorfer K, Flohr T. Spatio-temporal filtration of dynamic CT data using diffusion filters. In: Samei E, Hsieh J, eds. Proceedings of SPIE: medical imaging 2009-physics of medical imaging. Vol. 7258. Bellingham, WA: SPIE–-The International Society for Optical Engineering; 2009. pp. 725810–57.
22. Shrimpton PC, Hillier MC, Lewis MA, Dunn M. National survey of doses from CT in the UK: 2003. Br J Radiol 2006;79:968–80. doi: 10.1259/bjr/93277434
23. Blankstein R, Shturman LD, Rogers IS, Rocha-Filho JA, Okada DR, Sarwar A, et al. Adenosine-induced stress myocardial perfusion imaging using dual-source cardiac computed tomography. J Am Coll Cardiol 2009;54:1072–84. doi: 10.1016/j.jacc.2009.06.014
24. Ko SM, Choi JW, Song MG, Shin JK, Chee HK, Chung HW, et al. Myocardial perfusion imaging using adenosine-induced stress dual-energy computed tomography of the heart: comparison with cardiac magnetic resonance imaging and conventional coronary angiography. Eur Radiol 2011;21:26–35.
25. George RT, Arbab-Zadeh A, Miller JM, Kitagawa K, Chang HJ, Bluemke DA, et al. Adenosine stress 64- and 256-row detector computed tomography angiography and perfusion imaging: a pilot study evaluating the transmural extent of perfusion abnormalities to predict atherosclerosis causing myocardial ischemia. Circ Cardiovasc Imaging 2009;2: 174–82.
26. George RT, Arbab-Zadeh A, Miller JM, Vavere AL, Bengel FM, Lardo AC, et al. Computed tomography myocardial perfusion imaging with 320-row detector computed tomography accurately detects myocardial ischemia in patients with obstructive coronary artery disease. Circ Cardiovasc Imaging 2012;5:333–40.
27. Meyer M, Nance JW Jr, Schoepf UJ, Moscariello A, Weininger M, Rowe GW, et al. Cost-effectiveness of substituting dual-energy CT for SPECT in the assessment of myocardial perfusion for the workup of coronary artery disease. Eur J Radiol 2012;81:3719–25. doi: 10.1016/j.ejrad.2010.12.055
28. Tamarappoo BK, Dey D, Nakazato R, Shmilovich H, Smith T, Cheng VY, et al. Comparison of the extent and severity of myocardial perfusion defects measured by CT coronary angiography and SPECT myocardial perfusion imaging. JACC Cardiovasc Imaging 2010;3:1010–9. doi: 10.1016/j.jcmg.2010.07.011
29. Engel KJ, Herrmann C, Zeitler G. X-ray scattering in single- and dual-source CT. Med Phys 2008;35:318–32.
30. Petersilka M, Stierstorfer K, Bruder H, Flohr T. Strategies for scatter correction in dual source CT. Med Phys 2010;37: 5971–92.
31. Geleijns J, Joemai RM, Dewey M, de Roos A, Zankl M, Cantera AC, et al. Radiation exposure to patients in a multicenter coronary angiography trial (CORE 64). AJR Am J Roentgenol 2011;196:1126–32. doi: 10.2214/AJR.09.3983
32. Nakauchi Y, Iwanaga Y, Ikuta S, Kudo M, Kobuke K, Murakami T, et al. Quantitative myocardial perfusion analysis using multi-row detector CT in acute myocardial infarction. Heart 2012;98:566–72. doi: 10.1136/heartjnl-2011-300915